

Local detection of spin-orbit splitting by scanning tunneling spectroscopy

Christian R. Ast,^{1,2,*} Gero Wittich,² Peter Wahl,² Ralf Vogelgesang,² Daniela Pacil ,^{1,3} Mihaela C. Falub,¹ Luca Moreschini,¹ Marco Papagno,^{1,3} Marco Grioni,¹ and Klaus Kern^{1,2}

¹*Ecole Polytechnique F d rale de Lausanne (EPFL), Institut de Physique des Nanostructures, CH-1015 Lausanne, Switzerland*

²*Max-Planck-Institut f r Festk rperforschung, 70569 Stuttgart, Germany*

³*INFN and Universit  degli studi della Calabria, 87036 Rende, Cosenza, Italy*

(Received 22 March 2007; published 2 May 2007)

We demonstrate that the spin-orbit coupling of two-dimensional surface states can be detected locally by scanning-tunneling spectroscopy (STS). The spin splitting of the surface state induces a singularity in the local density of states which can be detected as a distinct peak in the differential conductance spectrum. From the STS spectrum we can determine the Rashba energy as a measure of the strength of the spin splitting. Its detection and imaging are demonstrated for the surface alloys Bi and Pb on Ag(111), which exhibit particularly large spin-split band structures. The influence of the spin splitting on the surface-state STS spectra of close-packed noble metal surfaces is also discussed.

DOI: 10.1103/PhysRevB.75.201401

PACS number(s): 68.37.Ef, 73.20.At, 79.60.-i, 71.70.Ej

Spin-orbit coupling is known to lift the spin degeneracy in symmetry-broken environments. Such spin-split surface states have been extensively studied in the past years, where angle-resolved photoemission spectroscopy (ARPES) has been the technique of choice because the spin-split bands exhibit a very characteristic dispersion.¹⁻⁵ However, ARPES is a real-space averaging technique and only sensitive to occupied states, so for a more complete picture local detection of the spin splitting as well as sensitivity in the unoccupied states is desirable. Scanning tunneling microscopy (STM) and spectroscopy are ideal techniques in this context, but their ability to detect spin-split bands has been in question for some time. Although the spin influences the quasiparticle interference,⁶ a statement about the strength of the spin splitting is seemingly impossible.⁷

In this Rapid Communication we show that by scanning tunneling spectroscopy (STS) it is possible to extract the strength of the spin splitting in a two-dimensional (2D) energy band from the local density of states (LDOS). Sub-monolayers of Pb or Bi on Ag(111) form long-range-ordered surface alloys, which exhibit particularly strongly spin-split 2D band structures, identified by ARPES, making them ideal candidates to demonstrate the local spin-splitting detection. Due to the different band occupation in the two systems, the singularity is either in the occupied [Bi/Ag(111)] or in the unoccupied [Pb/Ag(111)] state, both of which can be addressed by STS.

Figure 1(a) shows a topographic scan of the long-range-ordered hexagonal Bi/Ag(111) surface alloy (5   lattice constant) taken by STM.⁸ The alloy is grown by depositing one-third of a monolayer of bismuth onto a clean Ag(111) surface at a temperature of 400 K to yield a $\sqrt{3} \times \sqrt{3}R30^\circ$ reconstruction. The upper right inset shows a calculated topography which is superimposed onto the data.⁹ It shows that bright spots correspond to Bi atoms, each of which is surrounded by six Ag atoms, as indicated by the model in the lower right inset. A differential conductance (dI/dV) spectrum of the Bi/Ag(111) surface alloy measured close to the Fermi level by STS, which is related to the LDOS of the sample, is shown in Fig. 1(b). The spectrum shows an asymmetric peak near -130 meV. In the following we will show

that this peak is due to a singularity at a band onset in the LDOS resulting from a very strong spin splitting.

The corresponding band structure of the Bi/Ag(111) surface alloy measured by ARPES⁸ near the $\bar{\Gamma}$ point at the center of the surface Brillouin zone (SBZ) [Fig. 2(a)] shows two identical and nearly parabolic bands with a negative effective mass of $m^* = -0.31m_e$ and a band maximum at $E_0 = -0.118$ eV. Two blue parabolas are drawn as a guide to the eye. The bands replace the nearly-free-electron-like surface state of the bare Ag(111) surface and accommodate the p electrons donated by the Bi atoms. Their maxima are shifted away from $\bar{\Gamma}$ by an amount $k_0 = 0.13 \text{  }^{-1}$. This is a clear signature of the spin splitting induced by strong spin-orbit coupling in an environment with space inversion asymmetry.

These observations can be qualitatively understood on the basis of a simple nearly free electron model. The Hamiltonian describing the spin-orbit coupling at the surface is⁷ $H_{\text{SOC}} = \alpha_R (\vec{e}_z \times \vec{k}) \cdot \vec{\sigma}$ where α_R is the Rashba parameter which is proportional to an effective electric field. $\vec{\sigma}$ are the Pauli spin matrices. The vector \vec{e}_z is perpendicular to the surface, and $\vec{k} = (k_{\parallel}, k_{\perp})$ is the electron wave vector, with components parallel and perpendicular to the surface. The energy dispersion is $E(\vec{k}_{\parallel}) = \frac{\hbar^2}{2m^*} (k_{\parallel} \pm k_0)^2 + E_0$ where m^* is the effective mass

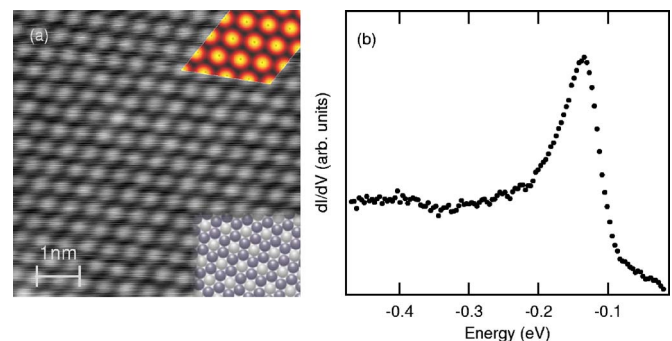


FIG. 1. (Color online) (a) Topography by STM of the long-range-ordered $\sqrt{3} \times \sqrt{3}R30^\circ$ Bi/Ag(111) surface alloy (bias voltage, -3 mV; tunneling current, 1 nA). (b) Local density of states measured by STS.

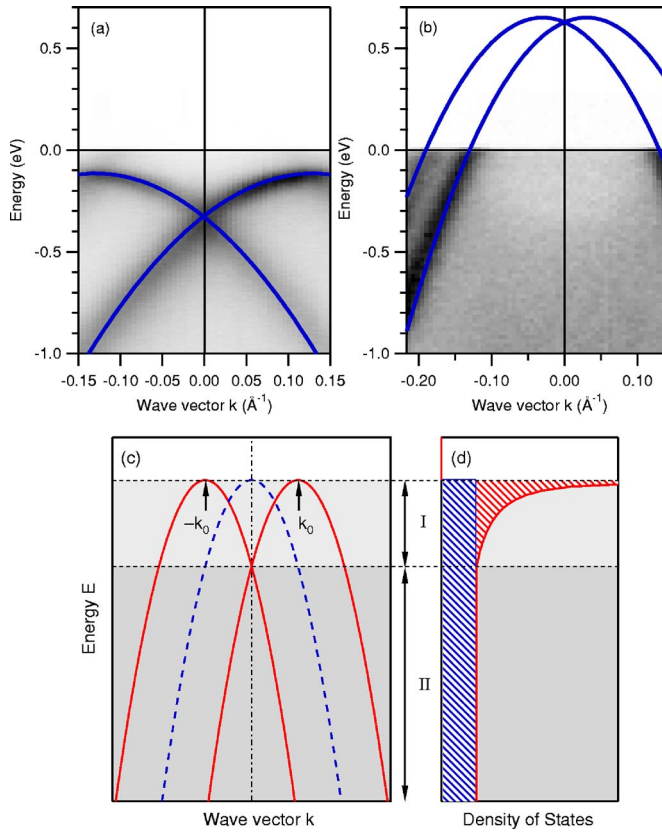


FIG. 2. (Color online) Band structure measurements by ARPES in the vicinity of the $\bar{\Gamma}$ point. The dispersion is traced by two blue (dark gray) parabolas to guide the eye. (a) Spin-split bands of the Bi/Ag(111) surface alloy with band maximum in the occupied states. (b) Spin-split bands of the Pb/Ag(111) surface alloy with band maximum in the empty states. (c) Calculated energy dispersion in the nearly free electron model with (red solid lines) and without (blue dashed line) spin-orbit coupling. (d) The corresponding density of states.

and $k_0 = m^* \alpha_R / \hbar^2$ is the offset by which the parabola is shifted away from $\bar{\Gamma}$. E_0 is an offset in energy. The energy dispersion is rotationally symmetric; it only depends on the magnitude of \vec{k}_\parallel .

Two qualitatively different energy regions can be identified which are detailed in Fig. 2(c). Regions I and II reach from the band maximum to the crossing of the two inner branches and from there to lower energies, respectively. The main difference between these regions concerns the density of states $D(E)$, which is easily evaluated analytically:

$$D(E) = \begin{cases} \frac{|m^*|}{\pi \hbar^2} \sqrt{\frac{E_R}{E - E_0}}, & E \in \text{region I,} \\ \frac{|m^*|}{\pi \hbar^2} = \text{const.}, & E \in \text{region II.} \end{cases}$$

This introduces a characteristic energy $E_R = \hbar^2 k_0^2 / 2m^*$ (also called Rashba energy¹⁰) which is related to the strength of the spin splitting. The DOS in Fig. 2(d) is constant in region II like in the two-dimensional free electron model without

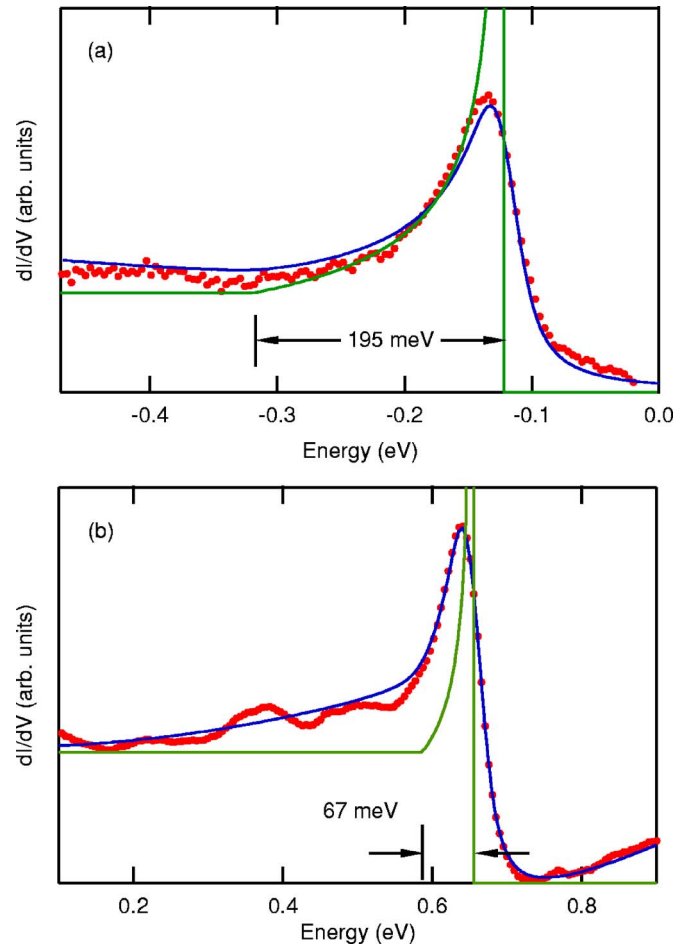


FIG. 3. (Color online) Differential conductance spectra near the surface-state onsets for different systems: (a) Bi/Ag(111) surface alloy and (b) Pb/Ag(111) surface alloy. The red dotted lines correspond to the measured dI/dV spectra, while the blue (dark gray) lines show a fit to the density of states within the Tersoff-Hamann model. The green (light gray) lines show the unconvoluted density of states.

spin-orbit splitting. In region I it follows a $1/\sqrt{E}$ behavior reminiscent of the Van Hove singularity in one-dimensional models. This is a signature of the spontaneous symmetry breaking which occurs for any finite k_0 turning the zero-dimensional pointlike band maximum for $k_0=0$ into a quasi-one-dimensional ringlike maximum. The width of region I is just the characteristic energy E_R .

The singularity at the band edge is a distinct feature of a spin-split band in a two-dimensional electron gas (2DEG). The finite lifetime and experimental broadening reduce the singularity to an asymmetric peak. This introduces a useful method for studying the spin splitting of energy bands by STS on a local scale. The experimental dI/dV spectrum near the band maximum of Bi/Ag(111) is shown in Fig. 3(a) as a red dotted line. The dI/dV spectrum has been fitted by a simulated STS spectrum—blue (dark gray) line—within the Tersoff-Hamann model¹¹ taking into account the transmission probability¹² and a finite linewidth. We calculate the lock-in derivative of the current with the modulation used in the experiment.¹³ The fit interval ranges over the full energy

window, which is visible in the respective graph. From the fit, we obtained the characteristic energy scale E_R of the spin-orbit splitting and an estimate of the lifetime of holes Γ_L at the Γ point. The Lorentzian broadening Γ_L is 40 meV, and the characteristic energy is $E_R=195$ meV [indicated by arrows in Fig. 3(a)].¹⁴ For comparison the unconvoluted density of states has been drawn as a green (light gray) line with the same parameters from the fit. Using the effective mass and the momentum offset from the ARPES data in Fig. 2(a) we find a characteristic energy of $E_R=208$ meV, which is in very good agreement with the STS results.

A very similar situation presents itself for the Pb/Ag(111) surface alloy. A third of a monolayer of Pb on Ag(111) forms the surface alloy structure as Bi/Ag(111) [see Fig. 1(a)].¹⁵ However, Pb has one valence electron fewer than Bi so that from a rigid band shift model we expect a very similar band structure except that the band maximum is shifted into the unoccupied states. In Fig. 3(b) the dI/dV spectrum of the Pb/Ag(111) surface alloy (red dots) shows a very similar onset with a rather sharp asymmetric peak located at $E_0=654$ meV. Due to the similarities between the Bi/Ag(111) and Pb/Ag(111) surface alloys, we infer a spin-split band structure and associate the peak with the characteristic divergence of the density of states. We have fit this spectrum to the above model, yielding a characteristic energy $E_R=67$ meV and a Lorentzian broadening $\Gamma_L=32$ meV with a lock-in broadening of 20 meV.

The experimental band structure of Pb/Ag(111) measured by ARPES is shown in Fig. 2(b). Away from the $\bar{\Gamma}$ point it shows two bands dispersing in parallel with a negative effective mass indicating a spin-split band structure. Two blue parabolas shifted in momentum by $k_0=0.03 \text{ \AA}^{-1}$ with the band maximum taken from the STS data and an effective mass of $m^*=-0.15m_e$ are superimposed onto the data to guide the eye. From these parameters we calculate a characteristic energy $E_R=23$ meV. This value is smaller than what has been found in the STS spectrum. However, since the exact dispersion in the unoccupied states is unknown, this value is an estimate only. Nevertheless, we can confirm that the peak in the Pb/Ag(111) dI/dV spectrum can be associated with the singularity in the density of states as a result of spin splitting.

Another system with strong spin-orbit coupling in an environment with space inversion asymmetry is the spin-split surface state on Au(111). The Au(111) surface state has been used in many instances as a model system for a spin-split surface state as, for example, the spin splitting is clearly visible in ARPES spectra.¹⁶ Compared to the Bi/Ag(111) surface alloy, however, the splitting is about an order of magnitude weaker. With a momentum offset $k_0=0.012 \text{ \AA}^{-1}$ and an effective mass of $m^*=0.26m_e$,¹⁷⁻¹⁹ we can calculate a characteristic energy E_R of only 2.1 meV. This is a rather small value, resulting in a very narrow region I. The lifetime broadening for the Au(111) surface state has been found to be 18 meV,¹⁹ a value that is almost an order of magnitude larger than the Rashba energy. Therefore, no signature of this singularity will be present in the differential conductance spectra on Au(111) measured by STS as model calculations have shown. The reason why it is nonetheless visible in

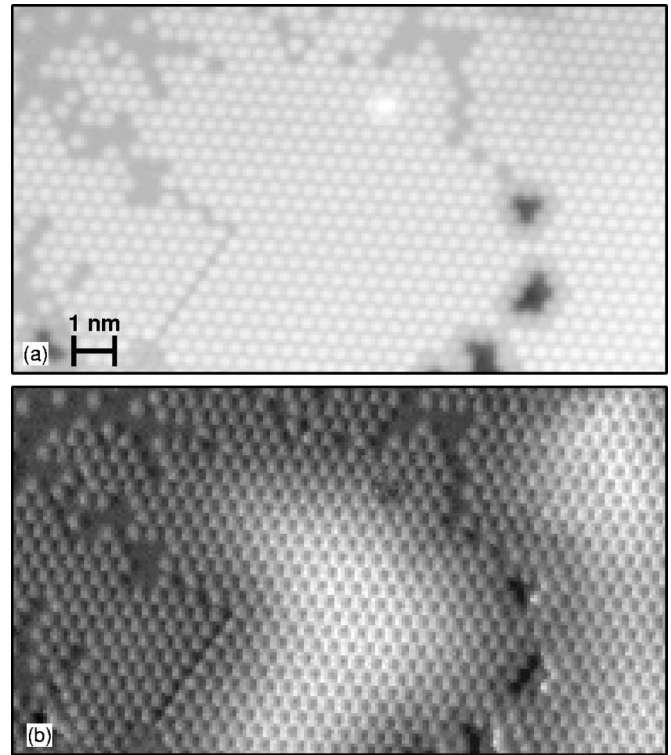


FIG. 4. (a) Topography of the Bi/Ag(111) surface alloy measured at a bias voltage of -0.137 V in a region with smaller island sizes. The bright spots are associated with Bi atoms. (b) Simultaneously acquired dI/dV map. Bright areas indicate a strong spin-split peak. Toward the island boundaries the peak vanishes.

ARPES spectra can be attributed to the momentum-dependent energy separation of the spin-split bands: As the momentum increases the energy separation will eventually exceed the lifetime broadening, making the separation visible in ARPES spectra. As a general rule, the spin splitting should be observable in the local density of states if the Rashba energy is larger than the intrinsic lifetime broadening.

In Fig. 4(a) an STM topography of the Bi/Ag(111) in a region with defects and domain boundaries is displayed. The protrusions can be associated with Bi atoms while the gray areas are the Ag(111) substrate. Three islands can be distinguished which are separated by domain walls. Figure 4(b) shows a dI/dV map which has been acquired simultaneously with the topography in Fig. 4(a) at a bias voltage of -0.137 V (peak maximum). The highest intensities appear as white in the image. We see that the peak is most pronounced in the center of the two larger islands while diminishing within a region of three to four lattice constants towards the island boundary. The small island on the left side does not show the high intensities at all. This demonstrates the ability to locally map the spin splitting in heterogeneous environments.

To better illustrate the spatial evolution of the spin-splitting singularity Fig. 5 shows a line scan of dI/dV spectra across a surface alloy island. The topographic line profile of the island is superimposed onto the image with the borders marked by vertical lines. At the island boundaries no peak is

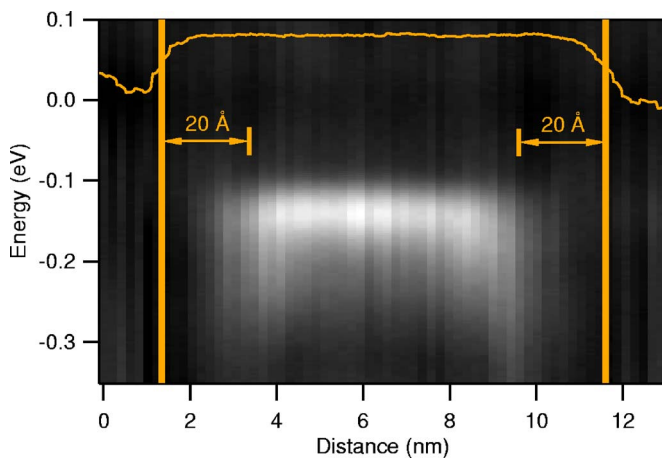


FIG. 5. (Color online) dI/dV spectra along a line across an alloy patch. The corresponding topographic line section (solid line) is superimposed onto the image with the borders marked as vertical lines. The peak intensity rapidly decreases near the border of the alloy patch.

observable. Towards the center of the island the peak develops within 20 Å of the island boundary. Figure 5 also shows that the peak becomes broader and the onset shifts slightly before the peak vanishes. The momentum broadening of 0.05 \AA^{-1} at $\bar{\Gamma}$ in the ARPES spectrum indicates a coherence length of about 20 Å supporting the observed length scale in the STS data. A possible explanation would be that, aside from geometrical effects,²⁰ the spin splitting changes near domain boundaries. Detailed scattering calculations are

needed to quantitatively model the effect of defects and domain boundaries.

In conclusion, we have demonstrated, using the Bi/Ag(111) and Pb/Ag(111) surface alloys, that the spin splitting of a surface state can be detected by scanning tunneling spectroscopy. It was necessary to use these systems for a proof of principle, because in the frequently used model system—the Au(111) surface state—the spin splitting is not strong enough to be detected in the local density of states. The ability to locally detect the spin splitting and extract its strength in the occupied as well as the unoccupied states nicely complements the capabilities of the ARPES technique. It opens new possibilities for a better understanding of the spin splitting in surface states and to address local variations.

An interesting application for the local detection of spin splitting can be found in the field of spintronics. It can be useful to create environments with locally varying spin splitting, as would be the case for a BiPb/Ag(111) mixed surface alloy with locally changing concentration. A recently proposed Stern-Gerlach spin filter²¹ uses a lateral voltage to create a locally changing spin splitting. The mixed surface alloy with a concentration gradient creates a static inhomogeneous spin splitting which would have the same effect as the proposed spin filter without the applied voltage.

We gratefully acknowledge L. Vitali and M. A. Schneider for help with the STS experiments as well as discussions with D. Malterre and H. Brune. P.W. acknowledges B. Hammer for his hospitality and stimulating discussions. C.R.A. acknowledges funding from the Emmy-Noether-Program of the Deutsche Forschungsgemeinschaft. The work at the EPFL was supported by the Swiss National Science Foundation through the MaNEP NCCR.

*Corresponding author. Electronic address: ast@fkf.mpg.de

¹S. LaShell, B. A. McDougall, and E. Jensen, Phys. Rev. Lett. **77**, 3419 (1996).

²J. Henk, M. Hoesch, J. Osterwalder, A. Ernst, and P. Bruno, J. Phys.: Condens. Matter **16**, 7581 (2004).

³D. Popović, F. Reinert, S. Hüfner, V. G. Grigoryan, M. Springborg, H. Cercellier, Y. Fagot-Revurat, B. Kierren, and D. Malterre, Phys. Rev. B **72**, 045419 (2005).

⁴H. Cercellier, Y. Fagot-Revurat, B. Kierren, F. Reinert, D. Popović, and D. Malterre, Phys. Rev. B **70**, 193412 (2004).

⁵F. Reinert, J. Phys.: Condens. Matter **15**, S693 (2003).

⁶J. I. Pascual, G. Bihlmayer, Yu. M. Koroteev, H.-P. Rust, G. Ceiballos, M. Hansmann, K. Horn, E. V. Chulkov, S. Blügel, P. M. Echenique, and Ph. Hofmann, Phys. Rev. Lett. **93**, 196802 (2004).

⁷L. Petersen and P. Hedegård, Surf. Sci. **459**, 49 (2000).

⁸The STM and STS measurements were done at 6 K in ultrahigh vacuum (1×10^{-10} mbar). The ARPES measurements were done at 300 K and at 77 K using 21.2-eV photons (He I) in ultrahigh vacuum (2×10^{-10} mbar). The energy and momentum resolution of the analyzer were better than 10 meV and $\pm 0.015 \text{ \AA}^{-1}$. Both experiments have *in situ* sample transfer and preparation.

⁹The calculation has been done with the DACAPO (<http://www.fysik.dtu.dk/CAMPOS/>) code using $12 \times 12 k$ points, a cutoff energy of 400 eV, and the PW91 functional and relaxing the structure. A six-layer slab has been used where the top layer was the alloy.

¹⁰D. S. Saraga and D. Loss, Phys. Rev. B **72**, 195319 (2005). The definitions of E_R differ by a factor of 2. We have chosen it to coincide with the width of region I.

¹¹J. Tersoff and D. R. Hamann, Phys. Rev. B **31**, 805 (1985).

¹²N. D. Lang, Phys. Rev. B **34**, 5947 (1986).

¹³J. Klein, A. Léger, M. Belin, D. Défourneau, and M. J. L. Sangster, Phys. Rev. B **7**, 2336 (1973).

¹⁴Other parameters in the fit were a tip-sample distance of 6 Å and a combined work function Φ ($\Phi = \Phi_{\text{sample}} + \Phi_{\text{tip}}$) of 10 eV.

¹⁵J. Dalmas, H. Oughaddou, C. Léandri, J.-M. Gay, G. Le Gay, G. Tréglia, B. Aufray, O. Bunk, and R. L. Johnson, Phys. Rev. B **72**, 155424 (2005).

¹⁶E.g., H. Cercellier, C. Didiot, Y. Fagot-Revurat, B. Kierren, L. Moreau, D. Malterre, and F. Reinert, Phys. Rev. B **73**, 195413 (2006); F. Forster, S. Hüfner, and F. Reinert, J. Phys. Chem. B **108**, 14692 (2004).

¹⁷F. Reinert, G. Nicolay, S. Schmidt, D. Ehm, and S. Hüfner, Phys. Rev. B **63**, 115415 (2001).

¹⁸G. Nicolay, F. Reinert, S. Hüfner, and P. Blaha, Phys. Rev. B **65**, 033407 (2001).

¹⁹J. Kliewer, R. Berndt, E. V. Chulkov, V. M. Silkin, P. M. Echenique, and S. Crampin, Science **288**, 1399 (2000).

²⁰O. Jeandupeux, L. Bürgi, A. Hirstein, H. Brune, and K. Kern, Phys. Rev. B **59**, 15926 (1999).

²¹J. I. Ohe, M. Yamamoto, T. Ohtsuki, and J. Nitta, Phys. Rev. B **72**, 041308(R) (2005).